catalysts

MDPI

Article

Rice Husk as an Inexpensive Renewable Immobilization Carrier for Biocatalysts Employed in the Food, Cosmetic and Polymer Sectors

Marco Cespugli [1], Simone Lotteria [1], Luciano Navarini [2], Valentina Lonzarich [2], Lorenzo Del Terra [2], Francesca Vita [3], Marina Zweyer [4], Giovanna Baldini [4], Valerio Ferrario [1], Cynthia Ebert [1] and Lucia Gardossi [1,*]

[1] Laboratory of Applied and Computational Biocatalysis, Dipartimento di Scienze Chimiche e Farmaceutiche, Università degli Studi di Trieste, Via Licio Giorgieri 1, 34127 Trieste, Italy; marco.cespugli@phd.units.it (M.C.); lotteria.simone@hotmail.it (S.L.); valerio.ferrario@gmail.com (V.F.); ebert@units.it (C.E.)

[2] illycaffè S.p.A., via Flavia 110, 34147 Trieste, Italy; luciano.navarini@illy.com (L.N.); valentina.lonzarich@illy.com (V.L.); lorenzo.delterra@illy.com (L.D.T.)

[3] Department of Life Science, University of Trieste, 34127 Trieste, Italy; vita@units.it

[4] Department of Medical, Surgical, and Health Sciences, University of Trieste, 34149 Trieste, Italy; marinazweyer@gmail.com (M.Z.); baldini@units.it (G.B.)

* Correspondence: gardossi@units.it; Tel.: +39-040-5583947

check for updates

Abstract: The high cost and environmental impact of fossil-based organic carriers represent a critical bottleneck to their use in large-scale industrial processes. The present study demonstrates the applicability of rice husk as inexpensive renewable carrier for the immobilization of enzymes applicable sectors where the covalent anchorage of the protein is a pre-requisite for preventing protein contamination while assuring the recyclability. Rice husk was oxidized and then functionalized with a di-amino spacer. The morphological characterization shed light on the properties that affect the functionalization processes. Lipase B from *Candida antarctica* (CaLB) and two commercial asparaginases were immobilized covalently achieving higher immobilization yield than previously reported. All enzymes were immobilized also on commercial epoxy methacrylic resins and the CaLB immobilized on rice husk demonstrated a higher efficiency in the solvent-free polycondensation of dimethylitaconate. CaLB on rice husk appears particularly suitable for applications in highly viscous processes because of the unusual combination of its low density and remarkable mechanical robustness. In the case of the two asparaginases, the biocatalyst immobilized on rice husk performed in aqueous solution at least as efficiently as the enzyme immobilized on methacrylic resins, although the rice husk loaded a lower amount of protein.

Keywords: covalent immobilization of enzymes; rice husk; polycondensation; CaLB; itaconic acid; aspartase; acrylamide; aspartase; renewable carriers; biomass

1. Introduction

Immobilized biocatalysts have the potential of enabling continuous processing, lowering production costs and waste stream generation. Moreover, prevention of protein contamination is one further motivation that induces food and cosmetic sectors to employ immobilized biocatalysts [1]. Nevertheless, immobilized enzymes represent only a minor fraction of the overall enzyme market and the number of immobilized enzymes used on a scale larger than 10 kton per year is limited [2]. The development of immobilized enzymes for applications in the food sector and in the production

of large volume chemicals must carefully consider both costs and sustainability issues. Inexpensive carriers and protocols, together with high reusability, are the factors that will determine the success of immobilized enzymes. Woodley and co-workers [3] demonstrated that, if considered a carrier with a cost of $50/kg, the carrier represents the largest contribution to the final cost, although the cost of some carriers available on the market for enzyme immobilization (e.g., methacrylic resins) can be 2–5 fold higher.

Furthermore, environmental factors and stringent regulations [4] are gaining increasing relevance in determining the overall viability of the biocatalytic process. Indeed, Life Cycle Analysis (LCA) [5] of biocatalyzed processes disclosed that the fossil-based raw materials of epoxy methacrylic resins represent the primary source of greenhouse gas emission for the immobilized enzymes. It is evident that in order to promote a wider uptake of immobilized enzymes for the production of high-volume and low-cost sustainable products, new carriers and immobilization strategies are needed [6].

Natural biopolymers from biomass represent attractive alternatives and on a global scale, the two highest-volume agricultural residues are rice husk (RH) and sugarcane bagasse [7]. Rice husk production accounts for around 120 Mt per year and only 20 Mt are currently used.

The literature reports a large number of studies where renewable materials or biopolymers have been used as economical and sustainable immobilization carriers [8] and recently we have also reported some preliminary results on the use of rice husk (RH) as a carrier for biocatalyst immobilization [9]. This natural and robust composite material is made of lignin, cellulose, hemicellulose and SiO_2 [10]. RH responds also to the pressing challenges of a circular economy, since it can be re-utilized at the end of its proposed industrial application [11]. Moreover, as natural composite material, it has the subsidiary advantage that it is subjected to less stringent legislative constraints even after chemical modification [12].

The milled RH requires minimal pre-treatment and it is applicable in both physical and covalent immobilization protocols and under various process conditions. Lipase B from *Candida antarctica* (CaLB), a protease and an invertase have been previously immobilized covalently on RH oxidized with $NaIO_4$ and functionalized with the spacer hexamethylenediamine (HMDA). The method exploits the nucleophilic reactivity of the lysine residues on the surface of the enzymes. Nevertheless, the low protein loading (<50%) indicated the need of further optimization. The present study addresses the problem of improving the percentage of protein loaded on the functionalized RH and aims at understanding the morphological factors that affect the chemical modification of this complex natural composite material. CaLB and two commercial asparaginases were selected for the immobilization and application of the biocatalysts in reaction of practical interest in solvent-free but also aqueous systems. The results here reported set the basis for the full exploitation of this versatile renewable biomass for the covalent anchoring of proteins and as functional material in general [13–16].

2. Results and Discussion

2.1. Morphological Characterization of the Rice Husk

The rice husk used in the present study derives from Italian rice varieties and its composition in terms of SiO_2, lignin cellulose and pentosanes was previously determined [10]. Figure 1 reports the Scanning Electron Microscopy (SEM) images of the entire cuticle of the RH before the milling.
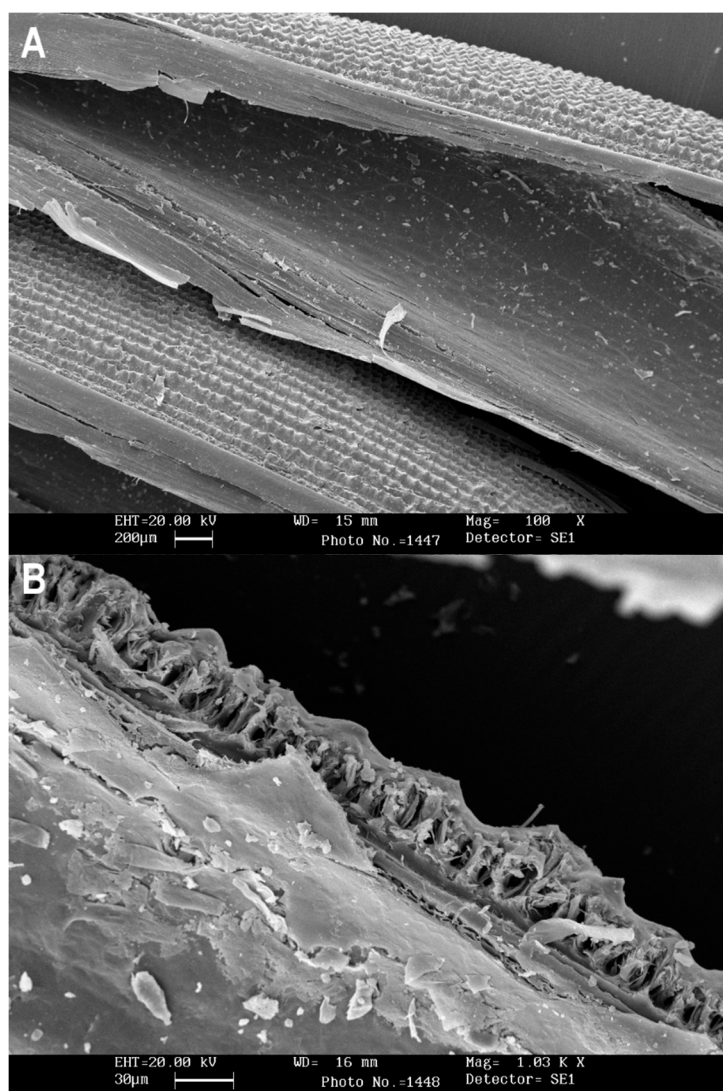
Figure 1. Scanning electron micrographs of rice husk fibers at different orders of magnification: (**A**) View of the external and internal surface; (**B**) internal section exposing the tracheids.

The rice husk has morphological differences between internal and external surfaces. The outer surface of the husk is very rough and presents linear ripples with a conical shape that run regularly along the whole surface. The outer surface contains a higher concentration of SiO_2 that confers stiffness and resistance towards external agents [17]. The internal surface, on the other hand, is smoother and consists of a larger quantity of cellulose.

The first step of the study was the detailed characterization of fractions of the milled RH differing in size (200–400 µm and 100–200 µm) using microscopy analysis (Figures 2–4). SEM microscopy (Figure 2) indicates that the material retains the typical morphology of the internal and external surface, probably because of the toughness conferred by the silica. Indeed, the milling of RH is feasible only by knife-mill devices whereas ball mill systems resulted inefficient. Therefore, most of the fragments expose only the lateral tubular structure as a result of the cutting of the stiff surface. Figure 2c,f provides details of the internal organization of RH, with the fibrous tubular structures of tracheids that form the mechanical skeleton of the material and have the function of transporting water and nutrients in the plant cell wall [18]. The matured dead plant cells retained only the lignocellulosic vascular structure.
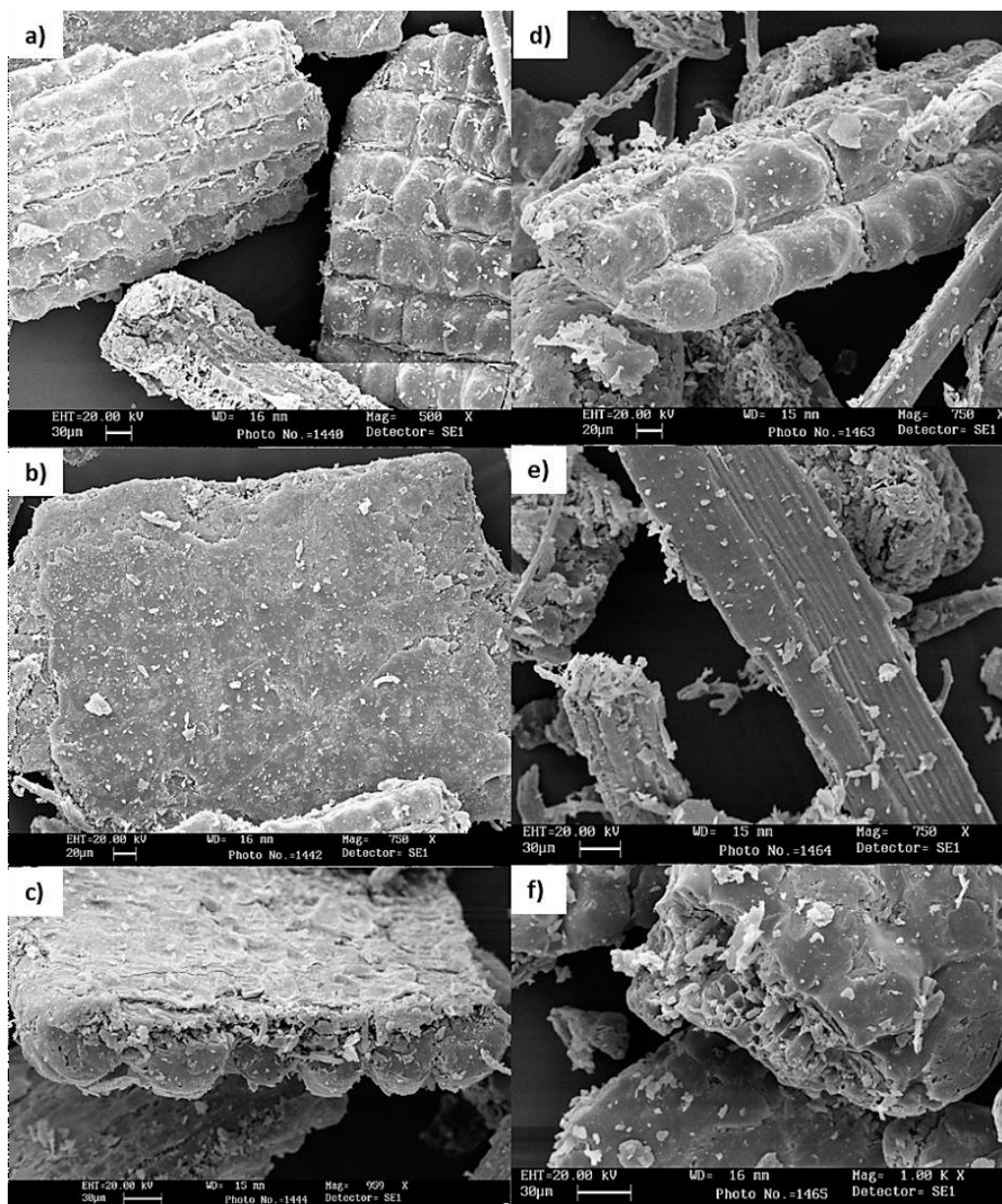
Figure 2. SEM images of: (**a–c**) Milled rice husk with particle size 200–400 μm; (**d–f**) milled rice husk with particle size 100–200 μm.

Bright field light microscopy (Figure 3) illustrates the tubular structures of tracheids and the external layer of SiO_2 that confers strength and rigidity to RH. Fluorescence microscopy (Figure 4a–c) shows how the material is endowed with autofluorescence especially in the blue (λ = 450–480 nm) and green range (λ = 510–520 nm). These are the typical wavelengths of the lignin, which composes the lignocellulosic biomasses [19]. Moreover, some restricted spots with autofluorescence in the red range (λ = 660–680 nm) are most probably ascribable to some residual chloroplasts [20]. Finally, the phase contrast image shows a single RH fragment that underwent a partial exposure of the inner cellulosic surface and highlights the regions where the lignin and the SiO_2 are more concentrated.
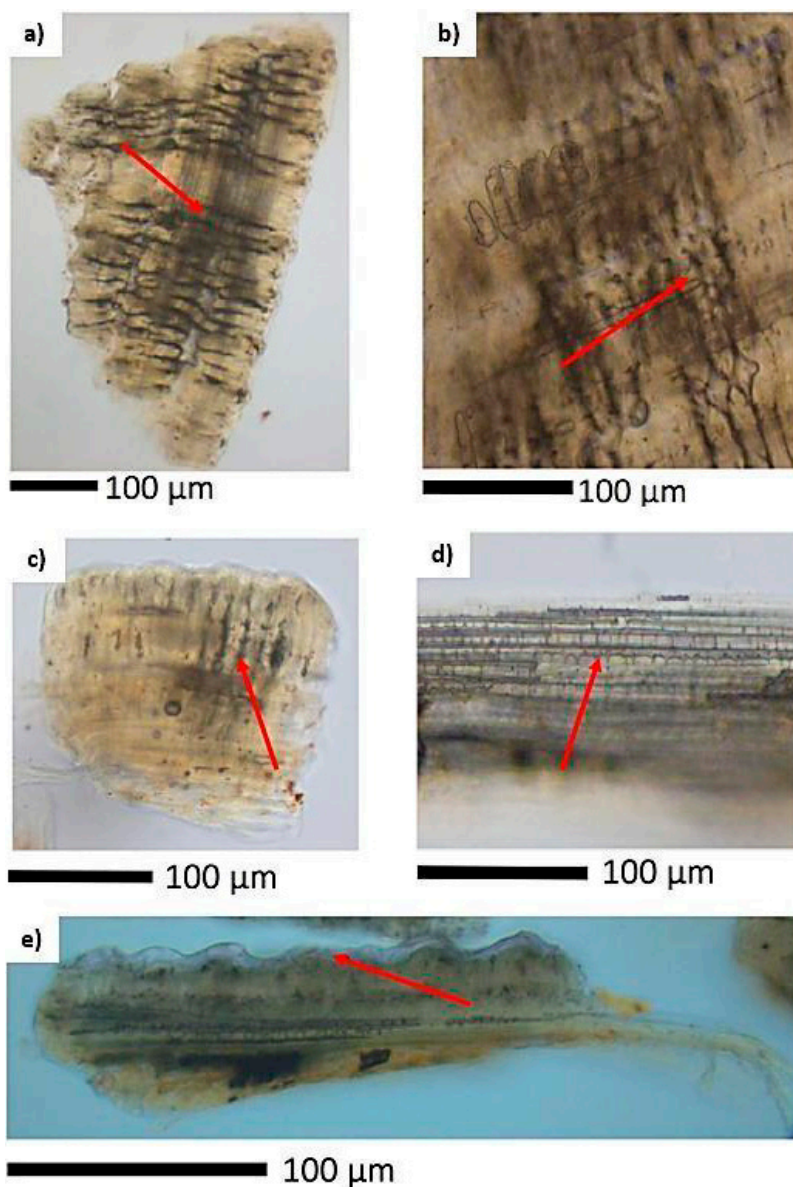
Figure 3. Bright field light microscopy images highlighting the tubular structure of tracheids (red arrows): (**a**,**b**) Milled rice husk (RH) with average size of 200–400 μm; (**c**,**d**) milled RH with average size of 100–200 μm; (**e**) detail of the external siliceous layer of a fragment of milled RH.
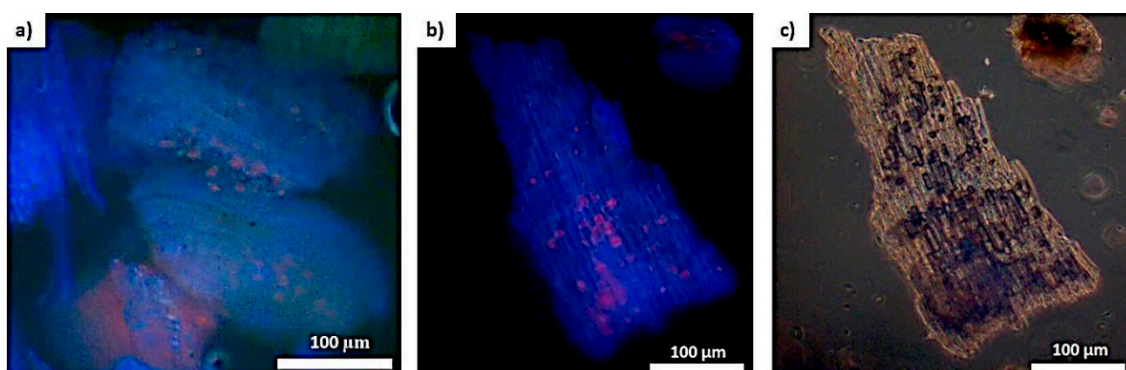

Figure 4. Milled RH (fragments with average size of 200–400 μm): (**a**,**b**) Fluorescence microscopy, (**c**) phase contrast image.

The data of mercury intrusion porosimetry (Table 1) indicates that the milling causes an increase of the porosity because of the exposure of the lignocellulosic tubular structures of tracheids.

Table 1. Comparison of porosity of RH before and after milling. Data were obtained by means of mercury intrusion porosimetry.

Material	Total Volume Intrusion (mL/g)	Total Pores Volume (m^2/g)	Average Pore Diameter (μm)	Porosity (%)
RH	0.2829	26.0	0.044	30.0
Milled RH (200–400 μm)	0.3889	17.3	0.090	37.9

Overall, the characterization of the RH and its fragments indicates that it is mandatory to increase the exposure of the lignocellulosic fraction of the tracheids in order to have access to a chemical substrate suitable for the derivatization and the covalent anchoring of proteins. The attack of the cellulosic component can occur at the level of the cut edges of the fragments or in regions that underwent the partial removal of the outer layer composed by lignin and SiO$_2$. It is also evident that the lignin fraction is poorly accessible due to the SiO$_2$ coating.

The activation of the surface was accomplished by oxidizing the cellulose with NaIO$_4$ as previously described [10]. The method preserves the glycoside bond while the oxidative cleavage of the glucose unit leads to a five-term di-aldehyde, which resemble in its chemical structure the glutaraldehyde, a largely employed reagent for the protein crosslinking as well as for enzyme immobilization (see Electronic Supplementary Information—ESI, Figure S1). Notably, reports on the use of oxidized carbohydrates for crosslinking established practical procedures, but never disclosed the molecular basis for the cross-linking of proteins. The formation of an imine-linkage with primary amino groups of Lys side chain was suspected to be the first step of the cross-linking by subsequent reductive amination [21]. In the case of dextran polyaldehyde, one-step cross-linking was first reported by Kobayashi and co-workers [22], demonstrating the possibility of obtaining rather stable products without reduction. Indeed, studies on the glutaraldehyde reactivity reported little or no reversibility of the imino bond formation within a pH range of 7–9 [23]. Moreover, the occurrence of unsaturated Michael addition products has been reported at basic pH [24].

The oxidation of RH [25] was carried out using the milled RH with a particulate size between 200 and 400 μm and the formation of the carbonyl groups was evaluated by titration (see ESI Figure S2) with hydroxylamine [26,27]. Moreover, the incidence of any subsequent oxidation of the carbonyl group to carboxylic acid was quantitatively evaluated (see ESI Figure S3) by means of a conductimetric titration [27,28]. The results obtained from the oxidation of the cellulose component of the rice husk by treatment with a 0.2 M NaIO$_4$ solution for 22 h are reported in Figure 5.

There is an increase of carbonyl groups of more than 380%, whereas carboxylic groups increase about 66%. Of course, some oxidative modification of the lignin cannot be excluded although the microscopic characterization indicates that SiO$_2$ covers most of the lignin, which appears poorly accessible (Figure 4).

2.2. Functionalization of RH with Amine Groups and Immobilization of CaLB

Upon oxidation of the cellulose, amine functional groups were inserted using hexamethylenediamine (HMDA) [10,29]. The functionalized RH was used for the covalent immobilization of CaLB, one of the most widely employed enzymes in oleo-chemical, cosmetic and food sectors. Its structure and superficial properties are illustrated in Figure 6.
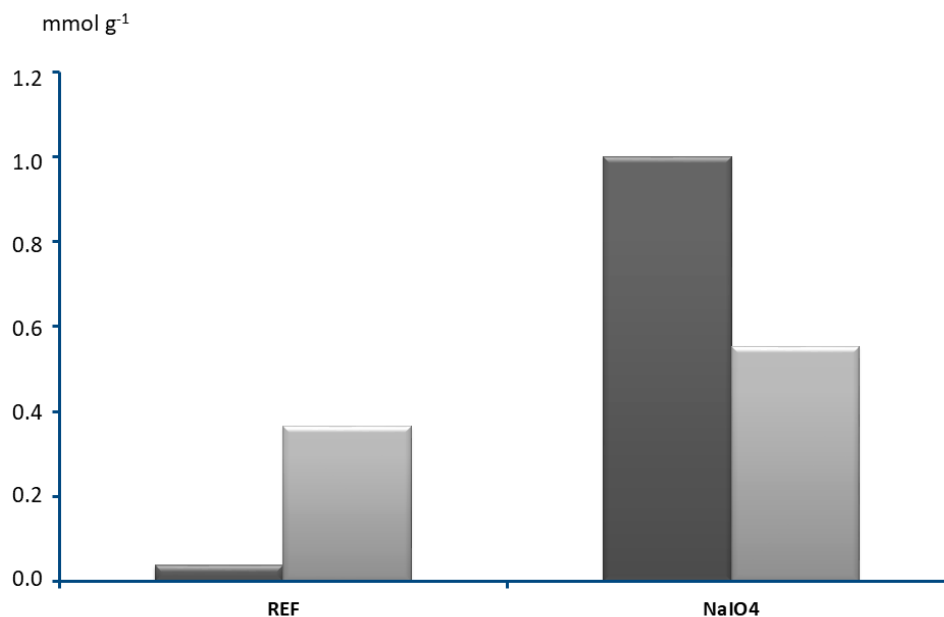
Figure 5. Comparison of the content (mmol·g^{-1}) of carbonyl (light gray) and carboxylic groups (black) in samples of milled RH before and after different oxidative treatment.
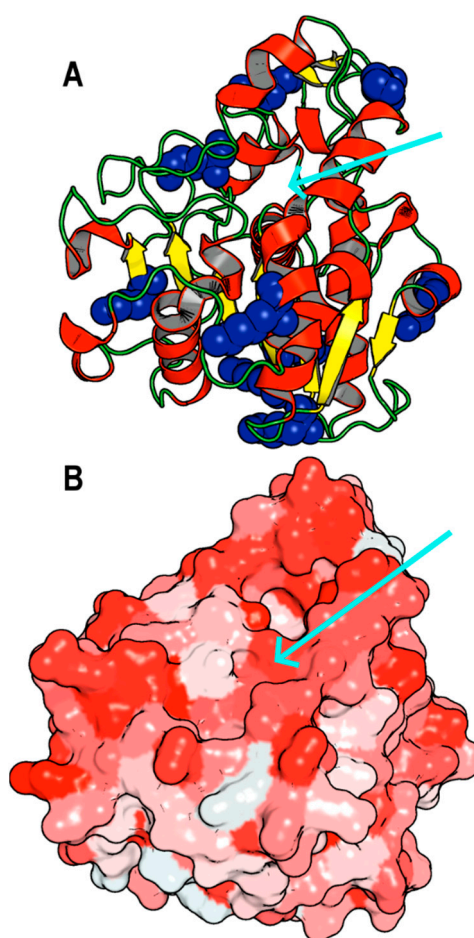

Figure 6. Analysis of the 3D structure of lipase B from *Candida antarctica* (CaLB, PDB: 1TCA). (**A**) The active site entrance is indicated by a cyan arrow while the superficial Lys are highlighted in blue spheres on the secondary structure of the enzyme. (**B**) The color of designates the hydrophobicity of the surface, going from white (hydrophilic) to red (hydrophobic).

Prior to lipase immobilization, the amine groups were activated for 5 h with a solution of glutaraldehyde (GA) in phosphate buffer. Finally, the activated carrier was incubated for 24 or 48 h in a solution of 10,000 U $g_{carrier}$ $^{-1}$ in 0.5 M phosphate buffer at pH 8 (Figure 7). A solution of PEG3000 was also added in order to improve the stability of the enzyme throughout the immobilization procedure [10]. The pH was selected in order to maintain deprotonated a sufficient fraction of the primary amine residues of the Lys thus allowing the reaction with the reactive groups present on the solid support. Moreover, the imine bond presents little or no reversibility as well the formation of Michael addition products [23].
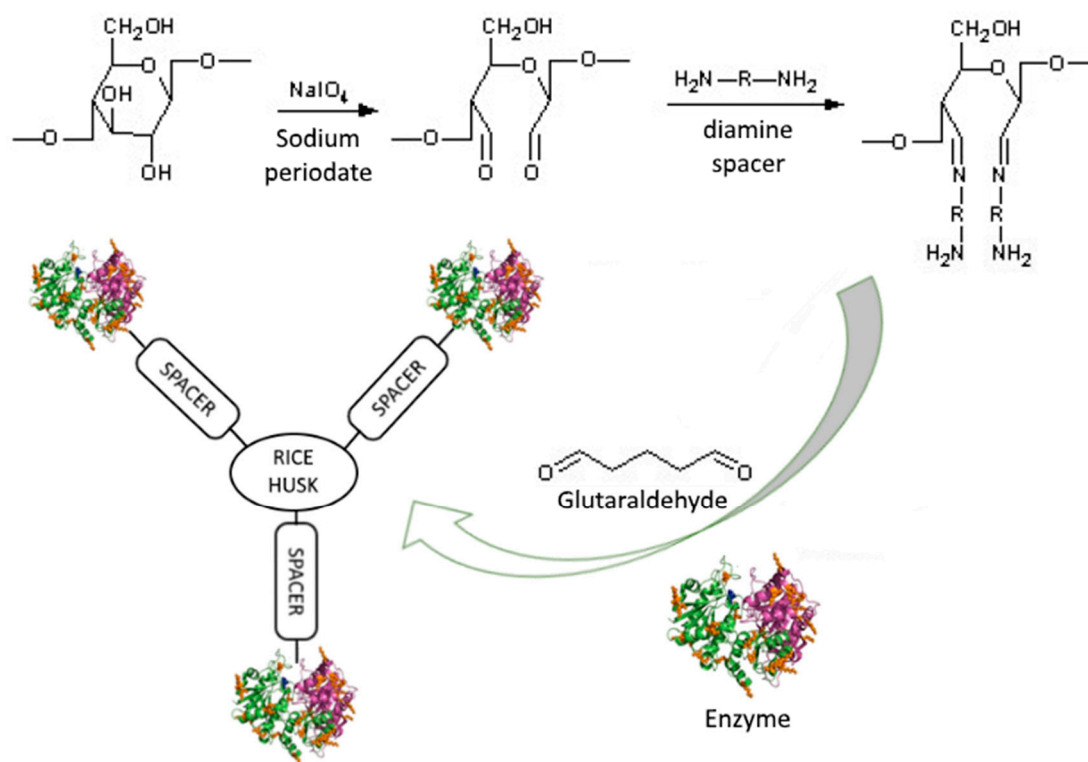

Figure 7. Schematic illustration of the oxidation and functionalization of the cellulosic fraction of RH for the covalent immobilization of CaLB.

In parallel, CaLB was also immobilized on the epoxy methacrylic resin EC-EP/S (size 100–300 μm). The actual anchorage of the CaLB through covalent bonding was verified for all immobilized biocatalysts by filtering the immobilized biocatalyst at the end of the hydrolytic assay and then by titrating the residual enzymatic activity in the supernatant using additional tributyrin. The data showed that no residual activity was detected in the filtered emulsion, as a proof that all the immobilized enzyme was covalently bound on the support (see ESI Figure S4). The recyclability of the CaLB immobilized on RH was also tested for 10 hydrolytic cycles (see ESI Figure S5) confirming the robustness of the formulation, as previously reported [9,10]. The properties of the different enzymatic formulations are reported in Table 2.

It is noteworthy that the extension of the immobilization time from 24 to 48 h led to an increase of the protein loaded on the RH from 33 to 72%. The need of a longer incubation time is ascribable to a slow adsorption of the enzyme to the RH [10], whereas it is widely demonstrated that the hydrophobic regions on CaLB induces a fast adsorption of the enzyme on hydrophobic organic resins [1]. Furthermore, the formation of the imino bond requires longer reaction times than the nucleophilic attack of the amine group to the epoxy ring of the EC-EP resins. Indeed, the loading of only 10,000 U of CaLB led to an expressed enzymatic activity of 316 tributyrin Units (TBU), comparable

to that previously reported by employing 25,000 U $g_{carrier}^{-1}$, and this result indicates that one gram of the functionalized RH carrier is already saturated with 10,000 U of CaLB.

Table 2. Properties of different formulations of covalently immobilized CaLB.

Carrier	Function Group	Immobilization Time (h)	Enzymatic U Loaded [a] (U $g_{carrier}^{-1}$)	Immobilized Protein [b] (%)	Hydrolytic Activity [a] (U g^{-1})
Oxidized Rice Husk	Amine (HMDA + GA)	24	25,000 [c]	35	317
Oxidized Rice Husk	Amine (HMDA + GA)	24	10,000	33	178
Oxidized Rice Husk	Amine (HMDA + GA)	48	10,000	72	316
Methacrylic EC-EP/S	Epoxy	24	10,000	95	709

[a] Units expressed as tributyrin hydrolytic activity referred to g of dry immobilized biocatalyst. [b] Amount of protein that was actually immobilized on the carrier, calculated by subtracting from the total amount of protein offered to the carrier the protein still present in solution at the end of the immobilization procedure. [c] Data previously reported [10].

Figure 8 reports a comparison of the morphology of the milled rice husk and the commercial epoxy activated methacrylic resins EC-EP/S (size 100–300 μm) that were selected for comparison. The milled RH has a very inhomogeneous morphology, with particles of various shapes.
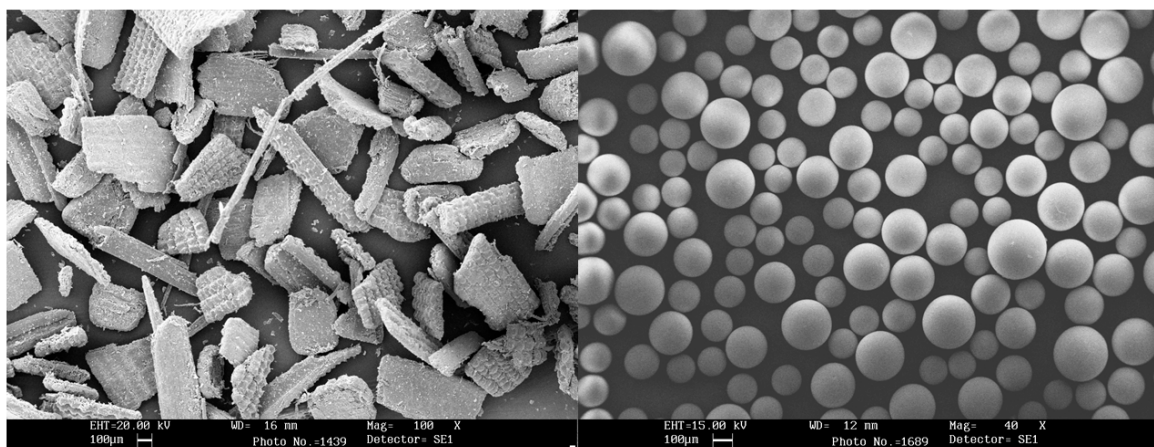

Figure 8. SEM images of: (**a**) Milled rice husk with average particle size 200–400 μm; (**b**) Sepabeads EC-EP epoxy methacrylic resin beads with average particle size 100–300 μm.

The comparison with a CaLB formulation prepared using a known procedure [10] and employing the commercial epoxy resin EC-EP/S (100–300 μm) shows that the epoxy group allows for faster immobilization protocols and, as expected, the percentage of loaded protein is close to 100% leading also to higher hydrolytic activities. The discrepancy between the two data obtained with EC-EP/S is due to the use of two different batches of the resin.

Despite the lower loading capacity, the functionalized RH is suitable for applications in bulk viscous polycondensation processes [30,31]. We have already demonstrated that the severe mass transfer limitations of these reactions can be overcome by maximizing the dispersion of the enzyme over a wide surface of the carrier rather than by increasing the loading of the biocatalyst. Moreover, any attempt to apply vigorous mixing systems while using methacrylic carriers resulted in the mechanical damage of the resins. In the present study, the polycondensation was carried out using a thin-film system that preserves the integrity of both the RH and the EC-EP resin [10,30,31].

The different formulations of covalently immobilized CaLB were used upon drying (see experimental) and in all cases, the water content of the formulations was <12% (*w/w*). Interestingly, despite the lower loading capacity, the RH-CaLB resulted more efficient in the solvent-free polycondensation of two bio-based monomers, dimethylitaconate (DMI) and 1,4-butandiol (BDO) to obtain poly(1,4-butylene itaconate) [30,31] (Figure 9 and Table 3). Enzymatically synthesized polyesters

with moderate MW are of interest for the cosmetic sector as film forming or for improving sensorial quality [32] but they find also applications as adhesives or pre-polymers prone to further chemical modifications [33,34]. More specifically, the derivatives of itaconic acid are gaining attention for the potential applications in dental materials, elastomers, drug-delivery and other biomedical and biotechnological applications [35]. Notably, the chemical polycondensation of itaconic acid leads to isomerization and radical cross-linking of the vinyl group under the conventional harsh reaction conditions (T > 150 °C). Therefore, the enzymatic polycondensation carried out at 50 °C appears as a convenient route for preserving the vinyl group throughout the synthetic process [31].
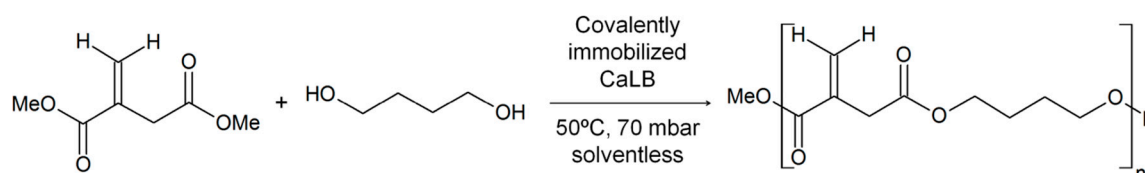

Figure 9. Solvent-free polycondensation catalyzed by CaLB covalently immobilized on RH.

The results in Table 3 and Figure 10 show that CaLB on rice husk and CaLB on methacrylic resin lead to comparable conversion and Mw values, although in the first case the polycondensation employed about half of the enzymatic units. The data indicate that the enzymatic preparation of CaLB on RH can be effectively employed for the sustainable synthesis of short bio-based polyesters with controlled structures. Nuclear Magnetic Resonance (NMR) characterization (see details in ESI Figures S6–S11) demonstrated that the enzymatic synthesis at 50 °C preserves all vinyl groups, thus making them available for further functionalization [31].

Table 3. Comparison of the results obtained by the polycondensation reaction catalyzed by the two different preparations of immobilized CaLB. Enzymatic units refers to tributyrin hydrolytic activity. Reaction were monitored by ^{1}H-NMR. Details are available in ESI.

Biocatalyst	U $g_{monomers}^{-1}$	Reaction Time (h)	Conversion (%)
CaLB RH	158	24	69
		48	87
		72	92
CaLB EC-EP/S	297	24	70
		48	87
		72	88

Notably, the use of a low amount of lipase (158 U $g_{monomer}^{-1}$) but dispersed on a wide amount of RH carrier (corresponding to 50% *w/w*) allowed also to overcome the low electrophilicity of the conjugated acyl group of the dimethylitaconate. Previously reported attempts [31] of synthetizing poly(1,4-butylene itaconate) using 240 U $g_{monomer}^{-1}$ of CaLB immobilized on EC-EP but concentrated in a smaller volume of carrier (10% *w/w*) led to the formation only of the trimer ABA where the diol (A) is acylated by the fast reacting carbons of two DMI units (B). Under such conditions only 5% of the slow reacting acyl group reacted, thus preventing the elongation of the polymeric chain.

One possible explanation of the higher efficiency of the RH as immobilization carrier resides in its lower density (0.4 g mL^{-1}) compared to methacrylic resins (>1.1 g mL^{-1} as stated by the producer). The two polycondensation reactions were carried out using an equal weight of the two immobilized formulations (50% *w/w* on monomers basis). Therefore, the volume available for the immobilization of the lipase is more than double in the case of RH. Indeed, the data confirm the previous observations [30] that mass transfer limitations can be overcome in viscous systems by distributing a limited amount of enzymatic units on a large volume of carrier. On that respect, the common paradigm of biocatalysis that calls for highly loaded and highly active biocatalysts appears not applicable to viscous systems.

Although the diameter of a single enzyme molecule is <10 nm and the pores of EC-EP/S (average pore diameter 10–20 nm), in principle, should be accessible to single enzyme molecules, the viscous reaction mixture has access only to the portion of CaLB immobilized on the outer surface of the carrier [30].
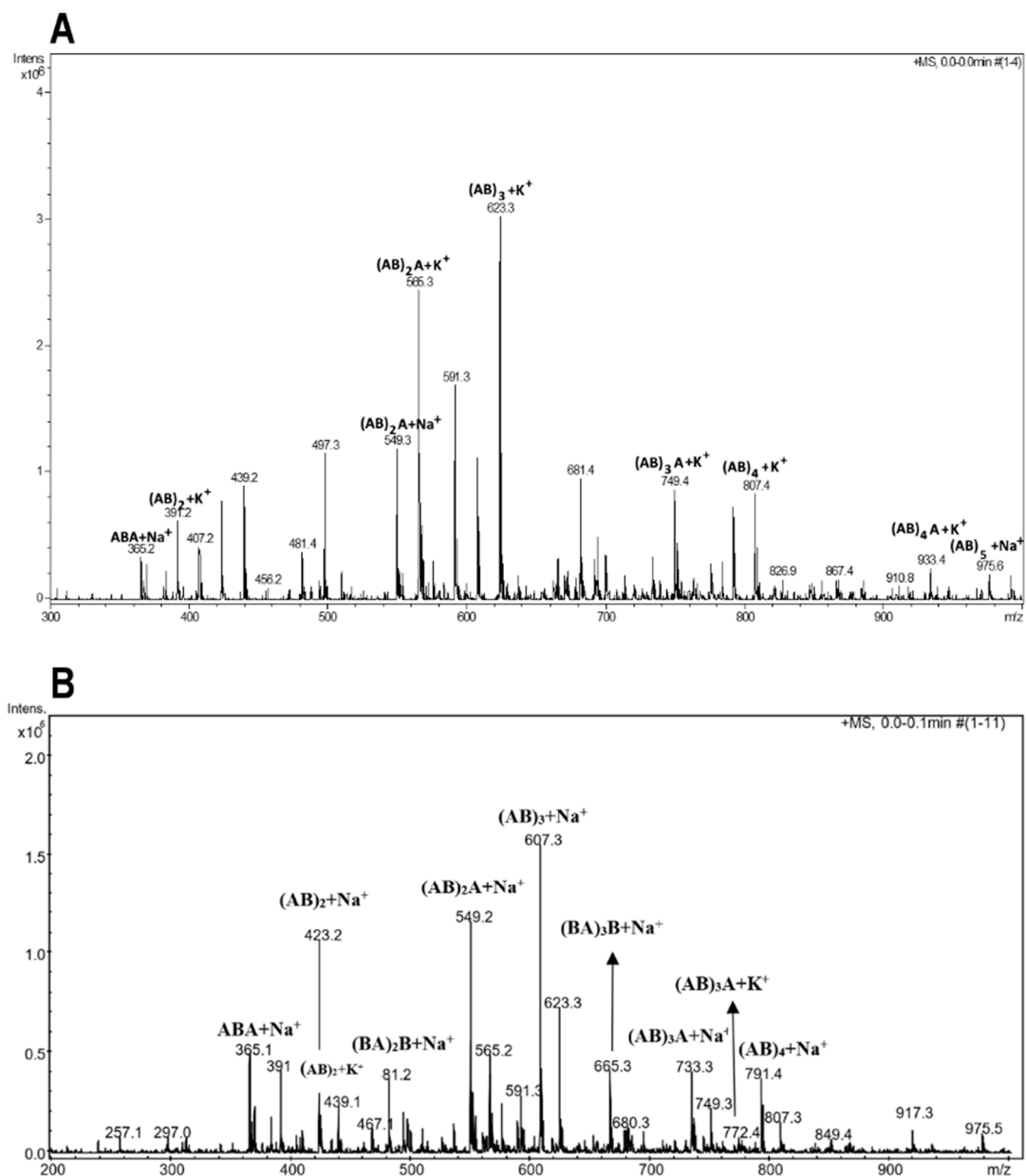

Figure 10. Electron Spry Ionization Mass Spectrometry (ESI-MS) positive ion mass spectra of the solvent-free enzymatic polycondensation products of dimethyl itaconate (DMI) with 1,4-butandiol (BDO) after 72 h. Top: Reaction catalyzed by CaLB on rice husk. Bottom: Reaction catalyzed by CaLB on EC-EP/S. A = BDO; B = DMI.

The role of the porosity of RH is more complex: Although the SEM images (Figure 2f) show that the opening of tracheids is quite wide (3–10 μm), these deep and straight channels (Figure 2e) are accessible only from the cut edges of the RH fragments. Therefore, this type of internal structure of RH (average pore diameter 90 nm, Table 1) is hardly comparable with the macroporosity of common silicate or methacrylic carriers. Further studies will be necessary for describing the localization of the enzymes molecules on the macropores of RH and also on its external surface.

For instance, Gross and co-workers analyzed by Infra Red (IR) imaging the localization of CaLB in Novozymes 435 [36], the biocatalyst most widely employed for polycondensation and made of a macroporous resin of poly-methyl methacrylate (Lewatit VP OC 1600). They showed that the protein is localized in an external shell of the bead with a thickness of 80–100 µm and that the distribution of CaLB is not uniform throughout this shell. However, in such case, the lipase was immobilized through physical adsorption, which makes the comparison with RH behavior even more difficult.

In order to evaluate the applicability of the CaLB covalently immobilized on RH, this formulation was also applied to the solvent-free synthesis of propyl laurate at 55 °C, a reaction system without relevant mass transfer limitations. In that case, the activity of CaLB-RH (expressed as µmol of propyl laurate formed by 1 g of immobilized biocatalyst in minute) was of 592 ± 24 µmol g^{-1} min^{-1}. The CaLB on EC-EP led to 2395 ± 41 µmol g^{-1} min^{-1}, demonstrating a higher efficiency of the mesoporous methacrylic resin in this kind of synthetic process. In conclusion, the efficiency of the two formulations of covalently immobilized CaLB depends strongly on the physical chemical properties of the reaction system.

2.3. Covalent Immobilization of Asparaginases on Functionalized Rice Husk

The study moved its focus to the application of functionalized RH as a carrier for the immobilization of asparaginases, which catalyze the hydrolysis of asparagine to aspartic acid. The enzyme is considered an effective means for reducing the formation of acrylamide in foods by degrading its precursor asparagine [37]. Upon heat treatments, asparagine undergoes condensation with reducing sugars then promoting a cascade of reactions that lead to the formation of acrylamide. Acrylamide is classified as "probably carcinogenic to humans" and the discovery of high levels of acrylamide in many common food products has intensified the research towards possible solutions of the problem [38] and to the development of commercially available food grade asparaginases enzymes.

Asparaginases are classified as asparagine starch hydrolase, namely amidases, with EC code (3.5.1.1.) The asparaginases from *Erwinia chrysanthemi* and *Escherichia coli* are currently in clinical use as effective drugs in the treatment of leukemia and several studies have already addressed the immobilization of asparaginases for clinical applications on supports such as magnetic nanoparticles [39], epoxy activated Sepharose [40] and protein micro particles [41]. The literature reports that asparaginases are tetramers of identical subunits, with molecular mass in the range of 140–160 kDa [41,42]. Each of the four active sites is located between the N- and C-terminal domains of two adjacent monomers. Thus, the tetramer can be treated as a dimer of dimers. Despite this fact, the active enzyme is always a tetramer. Each monomer consists of 327 residues. Therefore, the enzyme results to be rather large. Nine residues have been identified as essential within the active site because they are involved in substrate recognition and catalysis. The hydrolytic mechanism involves a residue endowed with nucleophilic activity (threonine 12 in the case of asparaginase from *Pyrococcus horikoshii*) within the active site [43].

The present study was carried out by combining the structural and functional analysis of two asparaginases commercialized by Novozymes. Acrylaway L is produced by the cloning of an asparaginase gene from *Aspergillus oryzae* in the same microorganism, although genetically modified, whereas Acrylaway High-T is obtained by cloning an unmodified gene into the genetically modified *Bacillus subtilis*. It must be noted that only the enzyme contained in the preparation Acrylaway L is potentially glycosylated as it is produced by a eukaryotic organism. The presence of large glycans (generally 8–30 units of mannoses) on the protein surface creates wide hydrophilic regions that affect the interactions of the enzyme with the outer environment or the immobilization carriers.

The two enzymes were evaluated in terms of protein concentration, presence of stabilizers, possible post-translational modifications (glycosylation) and all the factors that could influence their immobilization and final use. The asparaginases were immobilized covalently on RH and EC-EP/S resins to comply with EFSA (European Food Safety Authority) regulations regarding the use of

enzymes in food processing and more specifically the two asparaginases were immobilized covalently to guarantee the control of any contamination of the food by the enzyme [44].

The structure of the asparaginases from *Erwinia chrysantemi* was selected from the Protein Data Bank [45] as a model of reference for a general analysis of the structural features of asparaginases enzymes. Figure 11 shows the hydrophobic and hydrophilic areas of the protein surface, responsible for the preliminary physical interactions with the solid support and the distribution of the nucleophilic Lys residues, responsible for the covalent bonds with the carriers.
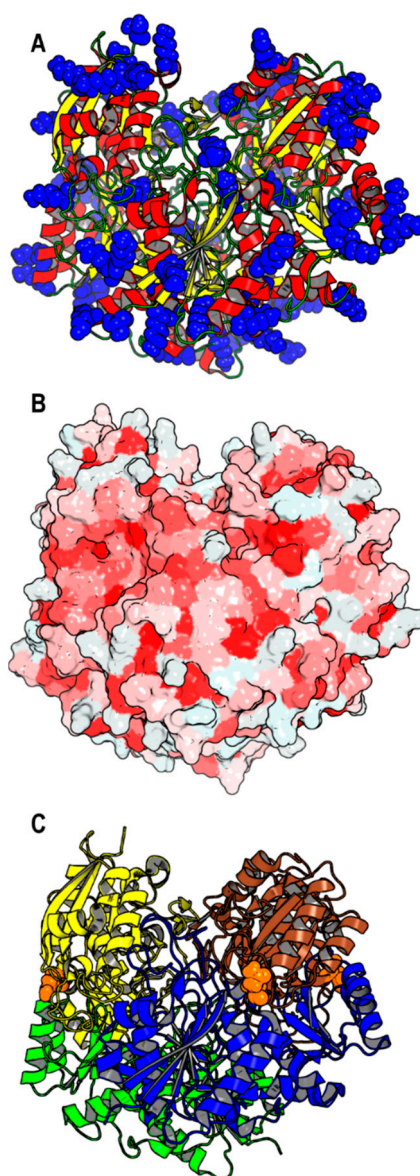

Figure 11. Analysis of the 3D structure of asparaginase from *Erwinia chrysantemi* in tetrameric form (PDB 1O7J). (**A**) The superficial Lys of the enzyme are highlighted in blue spheres on the secondary structure of the enzyme. (**B**) The colors of the enzyme surface indicate hydrophilic areas (white) and hydrophobic regions (red). (**C**) The tetrameric structure with each monomer colored differently while the glycosylation sites are highlighted in orange sphere mode.

The enzyme surface presents significant hydrophobic areas, which are generally absent in hydrolases such as proteases and amidases but widely present in lipases [46]. The potential N-glycosylation sites were also identified by analyzing the primary structure of the enzyme (see ESI Figure S12). They are located in each subunit (Figure 11C) in areas adjacent to the opening of the

active site. Generally, the glycans have the role of masking hydrophobic regions exposed to the bulk aqueous environment, thus preventing protein aggregation [47].

As illustrated in Figure 11, the enzyme has a large number of lysine residues and they are mostly disposed on the opposite side in respect to the opening of the active site. This element, although referred to a model structure, indicates that the asparaginase from *Erwinia chrysanthemi* is favorable for being covalently immobilized and achieving multi-point anchorage with correct orientation and free access to the active site.

The protocols for the covalent immobilization of the two asparaginases on the functionalized rice husk were developed by adjusting the two enzymatic solutions at the same protein concentration (3.40 mg/mL) to compare the affinity of the two enzymes for the carrier. The activity was tested for 10 cycles, in order to evaluate also the recyclability of the biocatalyst. The two asparaginases were also immobilized on EC-EP/S resins. The results of the characterization of the four preparations are reported in Table 4. Enzyme performance was determined by evaluating the amount of asparagine hydrolyzed by the immobilized enzymes after 30 min at 40 °C.

Table 4. Properties of the two asparaginase immobilized covalently on the functionalized rice husk and on EC-EP/S resins. The enzyme performance was determined by evaluating the amount of asparagine hydrolyzed after 30 min of incubation at 40 °C.

Carrier	Asparaginase	Loaded Protein ($mg \cdot g_{carrier}^{-1}$)	Actual Loaded Protein %	Actual Loaded Protein ($mg \cdot g_{carrier}^{-1}$)	Hydrolyzed Asparagine (%)	Hydrolyzed Asparagine after 10 Cycles (%)
EC-EP/S	Acrylaway L	26.8	72	12.3	100	100
	Acrylaway High-T	26.8	93	24.9	100	98.5
RH	Acrylaway L	17.9	44	7.9	100	100
	Acrylaway High-T	17.9	38	6.8	93	86.5

The different immobilization yields obtained with the two asparaginases indicates that the hydrophobic and hydrophilic interactions play important roles in favoring the initial adsorption of the enzyme on the support. Acrylaway L is a glycosylated asparaginase and therefore more hydrophilic. This characteristic translates in a lower immobilization yield on the methacrylic epoxy resin (72%) whereas the less hydrophilic Acrylaway High-T adsorbs and binds readily (93%) on the same hydrophobic resin. An opposite trend, although less marked, can be observed in the case of the immobilization on RH.

All immobilized biocatalysts expressed an excellent efficiency, especially those immobilized on rice husk that proved able to hydrolyze quantitatively the acrylamide in solution for 10 cycles of treatment. Notably, the amount of protein loaded on the methacrylic resins was about double as compared to the formulations obtained with RH. This indicates that the lower loading capacity of the functionalized RH is counterbalanced by an excellent dispersion of the light RH carrier in the aqueous solution and favorable access to the enzyme.

3. Materials and Methods

3.1. Materials

Samples of rice husk (*Carnaroli* type) were kindly donated by Riseria Cusaro (S.r.L.) (Binasco, Italy) and derive from Italian rice varieties. The organic composition, previously determined [10], is the following: 46.5% cellulose, 31.9% lignin and 22.1% of pentosans (hemicellulose). SiO_2 constitutes about 20% of the global weight. The milled RH has a water adsorption capacity of 42.6% *w/w*, determined by weight difference. Lipase B from *Candida antarctica* (CaLB, batch LCN02115 with an activity of 4005 U mL^{-1}), Asparaginases Acrylaway L (minimum activity stated by producer: 3500 ASNU/g) and Acrylaway High-T (minimum activity stated by the producer: 6000 TASU/g) were purchased from Novozymes (Bagsvaerd, Denmark). The protein content of Acrylaway L and

Acrylaway High-T, determined independently by the Bradford test using serum bovine albumin as standard, was 5.77 and 3.04 mg. mL^{-1} respectively. The solvents were standard laboratory grade. Alcohol, organic acid, and other reagents were purchased from either Aldrich Chemical Co. (Milwaukee, Wisconsin, United States) or Sigma-Aldrich (St. Louis, MO, USA) and used as received if not otherwise specified. Sepabeads EC-EP/S were purchased from Resindion (Milano, Italy). Product features as from the producer: Oxirane content: Minimum 100 μmol/g wet; Median pore diameter: 10–20 nm. Water retention: 55–65%.

3.2. Grinding and Sieving

Rice husk was milled using a Rotor mill ZM 200 (Retsch Cusaro (S.r.L.), Bergamo, Italy). The raw material was separated by size using four different sieves of 450, 250, 200 and 100 μm, respectively. The wet particles were weighed and then dried in an oven at 120 °C for 6 h. The density of RH before milling was 0.153 g mL^{-1} whereas the milled RH (size 0.2–0.4 mm) had a density of 0.437 g mL^{-1}. Porosity was determined using mercury porosimetry.

3.3. SEM Microscopy

Samples were metallized with the S150A Sputter Coater instrument (Edwards High Vacuum, Crawley, West Sussex, UK) before being observed with the Leica Stereoscan 430i scanning electron microscope (Leica Cambridge Ltd., Cambridge, UK) integrated with an Si detector (Li) PENTAFET PLUS TM, with an ATW TM window (Oxford Instruments, Oxfordshire, England) for microanalysis.

3.4. Light and Fluorescence Microscopy

Rice husk was put on glass slides, mounted with Canada balsam (Sigma-Aldrich, St. Louis, MO, USA) and kept under vacuum for a few minutes to remove air bubbles. Specimens for epifluorescence were mounted with glycerol and DABCO (1,4-Diazobicyclo-(2,2,2)octane (Sigma-Aldrich St. Louis, MO, USA).

Rice husk slides were observed with a Zeiss Axiophot microscope (Oberkochen, Germany) using transmission light or epifluorescence and micrographs were collected by a ProgRes CFcool camera (Jenoptic, Jena, Germany).

3.5. ^{1}H-NMR Spectra Related to Polycondensation of DMA and BDO

Spectra were recorded on a JEOL Ex-270 spectrometer (JEOL, Tokyo, Japan) operating (270 MHz). The solvent was CDCl$_3$ if not otherwise specified.

3.6. Thin Layer Chromatography (TLC)

Polycondensation was monitored on silica gel glass plates 20 × 20 cm (Macherey-Nagel, Düren, Deutschland). The spots were visualized by treating the silica plates with a solution mixture of KMnO$_4$/KOH (1.25/0.5%). The components were separated employing ethyl acetate as mobile phase.

3.7. Electrospray Ionization Mass Spectrometry (ESI-MS)

The crude reaction mixtures were analyzed on Esquire 4000 ESI-MS ion trap Bruker instrument (Karlsruhe, Germany) electrospray positive ionization by generating the ions in an acidic environment. Around 10 mg of sample was dissolved in 1 mL methanol containing 0.1% v. v^{-1} formic acid. The generated ions were positively charged with the m z^{-1} ratio falling in the range of 100–1000. The subsequent process of deconvolution allows the reconstruction of the mass peaks of the chemical species derived from the analysis of the peaks generated.

3.8. Moisture Determination

A sample of 1.0 g of rice husk (A) was weighed in a tarred weighing bottle. It was dried for 2 h in an oven at 105 ± 5 °C, cooled in a desiccator, and then the stopper was opened in order to equalize the air pressure and weigh. The bottle was replaced again in the oven for 1 h. The process was repeated, followed by cooling and weighing as above for successive periods until constant weight (B) was reached. Moisture content % = [(A − B)/A] × 100.

3.9. Titrations

Potentiometric titrations and pH measurements were performed using a Graphic DL50 Mettler Toledo automatic titrator. Conductimetric measurements were performed using a Conductivitymeter CDM 92 (Sigma-Aldrich St. Louis, MO, USA).

3.10. Lipase Hydrolytic Activity (Tributyrin Assay)

The activity of enzymatic preparations was assayed by following the tributyrin hydrolysis and by titrating, with 0.1 M sodium hydroxide (NaOH), the butyric acid that was released during the hydrolysis. An emulsion composed of 1.5 mL tributyrin, 5.1 mL gum arabic emulsifier (0.6% *w/v*) and 23.4 mL water was prepared in order to obtain a final molarity of tributyrin of 0.17 M. Successively, 2 mL of 0.1 M sodium-phosphate buffer (Nap), pH 7.0, was added to 30 mL of tributyrin emulsion and the mixture was incubated in a thermostatted vessel at 30 °C, equipped with a mechanical stirrer. After pH stabilization, 100 mg of immobilized biocatalyst or 0.005 mL CaLB native solution was added. The consumption of 0.1 M NaOH was monitored for 14 min. One unit of activity was defined as the amount of immobilized enzyme required to produce 1 μmol of butyric acid per min at 30 °C. One tributyrin unit (TBU) of lipase activity was defined as the amount of enzyme which liberated 1 μmol of butyric acid per minute under the given assay conditions.

3.11. Asparaginase Assay

L-Asparagine (Sigma A0884-25G, St. Louis, MO, USA) was dissolved in deionized water at a concentration of 100 mg L^{-1}. A total of 0.5 mg of immobilized asparaginase was added to 1 mL of this solution and was placed in 2 mL Eppendorf tubes. To obtain the previously mentioned amount of enzyme, 200 μL (volume of the storage buffer in which the immobilization matrix was carefully re-suspended) was used in the case of enzymes immobilized on resin. For enzymes immobilized on rice husks, the volume used was double (400 μL). After 30 min under stirring at 250 rpm on an orbital shaker at 40° C, the immobilized enzyme was recovered by centrifugation (Beckman-Coulter Allegra 64R centrifuge, Indianapolis, IN, USA, F2402H rotor, 17,000 rpm, 3 min, RT (21 °C)). At the end of the centrifugation, the concentration of asparagine was measured in the supernatant. Afterward, 1 mL of fresh asparagine solution was added to the precipitated enzyme for the next assay cycle. The procedure was repeated 9 times, for a total of 10 consecutive cycles of use of each enzyme sample. The determination of asparagine was carried out according to the procedures described by the EZ-faast® kit for amino acids (Phenomenex) by GC/MS Agilent Technologies (Santa Clara, CA, USA), equipped with a 10 m ZB-AAA capillary column, 0.25 mm thick film. A total of 100 μl of sample in the presence of 20 nmol of norvaline as internal standard were cleaned up through an ion exchange resin. The amino acids were released from the resin through *n*-propanol used as an eluting medium. The samples were then derivatized through propyl chloroformate, which allowed the alkylation of the amino and the esterification of the carboxylic group of each amino acid simultaneously. The sample preparation was in accordance with the procedures described by Phenomenex in the usage of the EZ-faast® kit for amino acids determination. Compounds were eluted by a He gas flow of 1 ml/min in splitless mode and separated using a 10 m ZB-AAA capillary column (film thickness 0.25 μm). The oven temperature was initially set at 110 °C, held for 1 min, increased to 160 °C at 25 °C/min, held for 1 min, then to 205 °C at a rate of 15 °C/min. The mass spectrometer was set to electron impact

mode (MS-EI) generated at 70 eV and mass spectra were collected in full scan mode, collecting ions from 39 to 500 m/z.

3.12. FT-IR

FT-IR spectra were recorded with a 2000 NIR FT-Raman spectrophotometer (Perkin Elmer, Roadgau, Germany). The samples, after drying in a desiccator, were reduced to powder with KBr and a tablet was prepared by pressing a force of 10 tons for 2 min. The spectra were recorded in a 4000–400 cm^{-1} spectral range and with a resolution of 2 cm^{-1}.

3.13. UV-Vis

UV-Vis spectra were recorded using a two-ray Lambda 35 spectrophotometer (Perkin Elmer, Rodgau, Germany) and a two-beam V-550 spectrophotometer (JASCO, Pfungstadt, Germany).

3.14. Determination of the Content of Carbonyl Groups

The content of carbonyl groups was determined by reaction with hydroxylamine chlorhydrate. This reacted with the hydroxylamine forming an oxime and the hydrochloric acid released was then titrated with sodium hydroxide. In 25 min of a 0.25 M solution of hydroxylamine and chlorhydrate, the pH was brought to 3.20 ± 0.05 with HCl. About 200 mg of rice husk of hydrated oxidized rice was added to the solution and the suspension was allowed to react for 2 h under stirring. After this time, the reaction was titrated with 0.1 M NaOH to bring the pH back to 3.20. At the end of the titration, the mixture was fed and the rice husk was dried for 6 h in an oven at 120 °C to determine the exact anhydrous weight of the analyzed sample.

To remove any interferences, a white consisting of a non-oxidized rice husk was treated with the same method, which was previously washed 6 times with an ethanol mixture:Water 50:50. Each measurement was performed twice. The content of carbonyl groups was calculated using the following formula:

$$\text{mmol aldehyde}/g_{carrier} = (V_{NaOH} \times C_{NaOH})/m_{dry\ carrier}$$

where V_{NaOH} is the volume in mL necessary to adjust the pH of the mixture to 3.20, C_{NaOH} is the concentration of NaOH (0.1 mmol/mL) and $m_{dry\ carrier}$ is the mass in grams of the anhydrous samples.

3.15. Determination of the Content of Carboxylic Groups with the Conductimetric Method

About 100 mg of sample was suspended in a beaker containing about 70 mL of 0.01 M HCl. The suspension was left under magnetic stirring for 30 min and subsequently titrated with 0.1 M NaOH. At the end of the titration, the suspension was filtered and the sample was dried for 6 h in an oven at 120 °C to determine the exact weight. As a reference, a solution consisting of 70 mL of 0.01 M HCl was titrated.

The content of carboxylic groups ($mmol_{COOH}/g_{sample}$) was determined with the following formula:

$$\text{carboxylic groups} = C_{NaOH} \times (V_1 - V_2)/m_{sample}$$

where CNaOH is the concentration of NaOH (0.1 mmol/mL), V_1 and V_2 are the volumes (mL) of NaOH necessary to control the weak acid present in the mixture (see ESI) and m_{sample} is the mass (g) of the anhydrous sample. The value of the carboxyl group contents was calculated on an average of two measures and it is reported with the standard deviation.

3.16. Oxidation of Rice Husk with Sodium Periodate

A total of 2 g of rice husk (particle size 200–400 μm) previously washed with a mixture of H_2O:ethanol 50:50 (3 × 3 mL) was placed in a syringe with septum. Then, 50 mL of a 0.20 M $NaIO_4$

solution was added and the mixture was allowed to react under stirring on the blood rotator for 22 h in the dark and at 25 °C. The solid support became dark brown. At the end of the reaction, the rice husk was filtered and rinsed with deionized water (3×10 mL) until neutrality.

3.17. Functionalization of Oxidized Rice Husk with HMDA Diamine Spacer

A total of 40 mL of a 0.9 M solution of hexamethylenediamine in methanol was added to the oxidized rice husk (200 mg) and the mixture was allowed to react for 72 h at 25 °C by stirring on the blood rotator. After this time, the rice husk was filtered and washed with methanol (2×40 mL).

3.18. Activation of Amine Functionalized Rice Husk with Glutaraldehyde Prior to Immobilization

Prior to immobilization, the amine-functionalized rice husk (200 mg) was activated by adding 50 mL of a 1.25% (v/v) glutaraldehyde solution in 0.05 M phosphate buffer at pH 8 and the suspension was allowed to react for 5 h at 25 °C. At the end of activation, the rice husk was filtered and washed with 0.05 M phosphate buffer at pH 8 (2×50 mL).

3.19. Determination of the Leaching of the Enzymes after Covalent Immobilization

At the end of the test for enzymatic activity, the biocatalyst was removed by filtration and 500 μL of the filtrate was taken, which were subjected to the enzymatic activity assay with tributyrin hydrolysis.

3.20. Immobilization of the CaLB on the Rice Husks Oxidized with Metaperiodate and Functionalized with Diamine Spacer

A total of 0.2 g of rice husk functionalized according to the procedure described above was placed in a syringe with septum. A 900 U/mL solution of Lipozyme CaLB was prepared in a vial by diluting the commercial preparation (4005 U/mL) in 0.5 M phosphate buffer at pH 8.

Immobilization was carried out by adding the enzymatic solution to the activate the rice husk to have a theoretical enzyme loading of 10,000 TBU $g_{carrier}^{-1}$. Then, 0.5 mL of a 2 mg/mL solution of PEG-3000 in phosphate buffer 0.5 M at pH 8 was added and the mixture was allowed to react at 25 °C on a rotating wheel for 24 or 48 h as stated in Table 2. After immobilization, the preparation was filtered and washed with 0.02 M phosphate buffer at pH 8 (6×1.2 mL), rinsed with acetone (4×1 mL) and dried on the septum of the syringe under vacuum (740 mbar). The preparation was transferred in a vial and stored in the fridge at 4 °C.

3.21. Immobilization of the CaLB on EC-EP/S Epoxy Methacrylic Resins

A total of 1.0 g of EC-EP/S epoxy resins (average particle size 100–300 μm) and washed once with 5 mL of deionized water were placed in a syringe with septum.

A 900 U/mL solution of Lipozyme CaLB was prepared in a vial by diluting the commercial preparation (4005 U/mL) in 0.5 M phosphate buffer at pH 8. Then, 11.4 mL of this solution was taken and added to the syringe containing the resin, so as to have a theoretical enzyme loading of 10,000 TBU $g_{carrier}^{-1}$. The mixture was allowed to react at 25 °C on a rotating wheel. After 24 h, the preparation was filtered and washed with 0.02 M phosphate buffer at pH 8 (6×3 mL). In order to quench the unreacted epoxy groups, the enzymatic preparation was incubated for 24 h with 15 mL of a saturated solution of glycine. Afterwards, the immobilized biocatalyst was filtered and washed with 0.02 M phosphate buffer at pH 8 (6×1 mL), then rinsed with acetone (3×3 mL) and dried on the septum of the syringe under vacuum (740 mbar for 30 min. The biocatalyst was transferred in a vial and stored at 4 °C.

3.22. Lipase Catalyzed Synthesis of Propyl Laurate

A total of 1.2 g of lauric acid (6 mmol) and 0.45 mL of 1-propanol (6 mmol) were placed in a 20 mL vial. The solution was thermostatted at 55 °C and kept under stirring (250 rpm) in an orbital shaker.

A sample (0.1 mL) was collected at t = 0 and weighed in a beaker. About 50 mg of biocatalyst were added to the initial solution and the mixture was left under stirring for 15 min. At regular intervals, 0.1 mL of the mixture were collected, weighed in a beaker and subsequently diluted in beakers with 7 mL of ethanol under continuous magnetic stirring. Three drops of phenolphthalein solution were added as an indicator. The samples were then titrated with a 0.1 M solution of KOH in ethanol until a persistent color change (light pink). The measurements were made in duplicate. One unit of activity (U/$g_{biocatalyst}$) of the biocatalyst is defined as the amount of immobilized enzyme necessary to produce 1 µmol of propyl laurate in one minute at 55 °C without solvent.

3.23. Solvent-Free Polycondensation of Dimethyl Itaconate with 1,4-butandiol Catalyzed by CaLB Immobilized on Epoxy Methacrylic Resins

A total of 16 mmol (2.4950 g) of dimethyl itaconate, 8 mmol (0.7310 g) of 1,4 butanediol and the immobilized enzyme (50% w/w; 297 U $g_{monomer}^{-1}$) were transferred to a 100 mL flask connected to a rotary evaporator at 200 rpm. A pressure of 70 mbar and a water bath temperature of 50 °C was applied. After 6 h, another 8 mmol of BDO were added and the mixture was left to react for 72 h. The enzyme was removed from the mixture by vacuum filtration and washing with dichloromethane. The solvent was subsequently removed under reduced pressure (600–500 mbar). The reaction product appears colorless and viscous. The characterization of the reaction product was carried out by 1H-NMR spectroscopy (see ESI) by dissolving the sample in deuterated chloroform (CDCl3) and by ESI mass spectrometry. The conversion was calculated by 1H-NMR, taking into account the signal relative to methylene in α to the hydroxyl in 1,4-butanediol and the signal of the same methylene in the esterification product [30]. The raw product was also solubilized in tetrahydrofuran (THF) and analyzed by Gel Permeation Chromatography (GPC).

3.24. Solvent-Free Polycondensation of Dimethyl Itaconate with 1,4-butandiol Catalyzed by CaLB Immobilized on Functionalized Rice Husk

A total of 8 mmol (1.2485 g) of dimethyl itaconate, 4 mmol (0.3600 g) of 1,4 butanediol and the immobilized enzyme (50% w/w; 158 U $g_{monomer}^{-1}$) was transferred to a 25 mL flask connected to a rotary evaporator at 200 rpm. The reaction was carried out as described in the paragraph above.

3.25. Lipase Hydrolytic Activity Assay for Determining Tributyrin Units (TBU)

The activity of enzymatic preparations was assayed by following the tributyrin hydrolysis and by titrating with 0.1 M sodium hydroxide (NaOH), the butyric acid that is released during the hydrolysis. An emulsion composed of 1.5 mL tributyrin, 5.1 mL gum arabic emulsifier (0.6% w v^{-1}) and 23.4 mL water was prepared in order to obtain a final molarity of tributyrin of 0.17 M. Successively, 2 mL of 0.1 M sodium-phosphate buffer (Nap) pH 7.0 was added to 30 mL of tributyrin emulsion and the mixture was incubated in a thermostatted vessel at 30 °C, equipped with a mechanical stirrer. After pH stabilization, 100 mg of immobilized biocatalyst or 0.005 mL CaLB native solution was added. The consumption of 0.1 M NaOH was monitored for 14 min. One unit of activity was defined as the amount of immobilized enzyme required to produce 1 mmol of butyric acid per min at 30 °C. One unit (U) of lipase activity was defined as the amount of enzyme which liberated 1 mmol of butyric acid per minute under the given assay conditions.

3.26. Immobilization of Acrylaway L on Activated Rice Husk

In order to exclude the protein concentration as a variable between the two asparaginase preparations, it was decided to operate Acrylaway L (5.77 mg/mL) at the same enzymatic concentration of Acrylaway High-T (3.04 mg/mL). In a vial containing 3.1 mL of Acrylaway L, corresponding to 17.9 mg $g_{carrier}^{-1}$, 1.25 mL of 2 mg/mL solution of PEG-3000 was added in 0.5 M of phosphate buffer at pH 8, and the pH was adjusted to 8 by adding, under stirring, 0.1 M NaOH. The enzymatic solution thus prepared was added to the syringe containing 0.5 g of functionalized rice husk and the mixture

was allowed to react at room temperature by stirring on the blood rotator. After 48 h, the preparation was filtered and washed with 0.02 M phosphate buffer at pH 8 (6 × 3 mL). The biocatalyst was transferred into a vial and suspended in a 70:30 mixture of glycerol: 0.02 M phosphate buffer at pH 8.

3.27. Immobilization of Acrylaway High-T on Activated Rice Husk

A total of 5.9 mL of Acrylaway High-T (26.8 mg of protein) was placed in a vial and 1.25 mL of a solution 2 mg/mL of PEG-3000 in 0.5 M phosphate buffer at pH 8 was added. The pH was adjusted to 8 by adding, under stirring, 0.1 M NaOH. The enzyme solution thus prepared was added in the syringe containing 0.5 g of rice husk functionalized as described above. The mixture was allowed to react at 25 °C by stirring on a rotating wheel. After 48 h the amount of immobilized protein (%) was determined and the preparation was filtered and washed with phosphate buffer 0.02 M pH 8 (6 × 3 mL). The biocatalyst was transferred into a vial and suspended in a 70:30 mixture of glycerol in 0.02 M phosphate buffer at pH 8.

3.28. Immobilization of Acrylaway L on EC-EP/S Resins

A total of 1 g of EC-EP/S epoxy resin (particle size 100–300 μm) was weighed in a test tube with filter. The resin was washed 3 times with 4 mL of deionized water. An enzymatic solution of Acrylaway L at a concentration of 3.4 mg/mL was prepared in a vial by adding 4.3 mL of 0.5 M phosphate buffer at pH 8 to 3.6 mL of Acrylaway L. The pH was adjusted to 8 by adding, under stirring, 0.1 M NaOH and the enzymatic solution thus prepared was added to the tube containing the resin. The suspension was allowed to react on a rotating wheel at 25 °C. After 24 h the preparation was filtered and washed with 0.02 M phosphate buffer at pH 8 (6 × 3 mL). The biocatalyst was transferred into a vial and suspended in a 70:30 mixture of glycerol:phosphate buffer of 0.02 M at pH 8.

3.29. Immobilization of Acrylaway High-T on EC-EP/S Resins

A total of 1 g of epoxy resin (particle size 100–300 μm) was weighed in a test tube with filter. The resin was washed 3 times with 4 mL of deionized water. Then, 7.7 mL of Acrylaway High-T (26.8 mg of protein) was added to a vial, the pH was adjusted to 8 by adding, under stirring, 0.1 M NaOH, and the thus prepared enzymatic solution was added to the test tube containing the resin. The immobilization was carried out as described in the previous paragraph.

3.30. Determination of Water Content in Enzymatic Preparations

A known amount of biocatalyst was placed on an aluminum plate and the sample was dried for 6 h in an oven at 120 °C. The water content (% w/w) was determined by determining the difference in weight before and after the drying procedure.

3.31. Computational Construction of 3D Models and Analysis of the Surface of Asparaginases

Protein structures were visualized and recorded using the PyMOL software (2.0 version). The 3D structures used for the hydrophobicity comparisons were retrieved from PDB. The representation and the calculation of the hydrophobic enzyme surfaces were performed by GRID mapping, using two different probes describing and quantifying different interactions: WATER (dipolar interactions and hydrogen bond formation), DRY (hydrophobic interactions) [46]. The N-glycosylation sites were determined using the open source software available at http://www.cbs.dtu.dk/services/NetNGlyc/. Details are available in the ESI.

4. Conclusions

In the present study, we have demonstrated the applicability of functionalized rice husk as a carrier for the covalent immobilization of lipase B from *Candida antarctica* (CaLB) and two asparaginases. This new renewable and inexpensive carrier, although not optimized, proved to be more efficient

than the fossil-based commercial methacrylic resins in the solvent-free synthesis of poly(1,4-butylene itaconate) catalyzed by CaLB. Although the micro-porosity of rice husk cannot be exploited for loading the enzymes, this composite material appears a suitable solution for highly viscous systems, having severe mass transfer limitations. Data demonstrate that, by dispersing the enzyme on the outer surface of a large volume of inexpensive carrier, the maximum mass transfer is achieved. Overall, the remarkable robustness of the milled RH associated with a low density (0.4 g mL^{-1} vs. 1.1 g mL^{-1} of methacrylic resins) appear as the main features that affect the performance of this renewable carrier. The functionalized rice husk was also efficiently used in aqueous solutions as carrier for asparaginases enzymes, which catalyzed the hydrolysis of the precursor of acrylamide, a toxic side product of various types of food. The covalently immobilized enzymes demonstrated optimal dispersibility and recyclability. The morphological characterization of RH provides the basis for further optimization studies. As appears from microscopy analysis, the cellulosic surface available for oxidation and further functionalization is rather limited in the milled rice husk. In addition, the lignin fraction is prevalently masked by a SiO$_2$ layer, which confers mechanical resistance to the material notwithstanding its very low density. The possibility of immobilizing enzymes on large volumes of inexpensive renewable carriers opens new perspectives for overcoming the environmental impact of fossil-based carriers, while boosting the economic viability of processes nowadays hampered by the high cost of immobilized biocatalysts.

References

1. Cantone, S.; Spizzo, P.; Fattor, D.; Ferrario, V.; Ebert, C.; Gardossi, L. Lipases for bio-based chemistry-Efficient immobilised biocatalysts for competitive biocatalysed processes. *Chem. Today* **2012**, *30*, 10–14. [CrossRef]
2. Di Cosimo, R.; McAuliffe, J.; Poulose, A.J.; Bohlmann, G. Industrial use of immobilized enzymes. *Chem. Soc. Rev.* **2013**, *42*, 6437–6474. [CrossRef] [PubMed]
3. Tufvesson, P.; Lima-Ramos, J.; Nordblad, M.; Woodley, J.M. Guidelines and Cost Analysis for Catalyst Production in Biocatalytic Processes. *Org. Process Res. Dev.* **2011**, *15*, 266–274. [CrossRef]
4. Liu, Y.; Andryszkiewicz, M.; Peña, R. Outcome of a public consultation on the draft Statement on Exposure Assessment of Food Enzymes. *EFSA Support. Publ.* **2016**, *13*, 1106E. [CrossRef]
5. Pellis, A.; Cantone, S.; Ebert, C.; Gardossi, L. Evolving biocatalysis to meet bioeconomy challenges and opportunities. *New Biotechnol.* **2017**, *40*, 154–169. [CrossRef] [PubMed]
6. Cantone, S.; Ferrario, V.; Corici, L.; Ebert, C.; Fattor, D.; Spizzo, P.; Gardossi, L. Efficient immobilisation of industrial biocatalysts: Criteria and constraints for the selection of organic polymeric carriers and immobilisation methods. *Chem. Soc. Rev.* **2013**, *42*, 6262–6276. [CrossRef] [PubMed]
7. Ravindran, R.; Jaiswal, A.K. Exploitation of food industry waste for high-value products. *Trends Biotechnol.* **2016**, *34*, 58–69. [CrossRef] [PubMed]
8. Sheldon, R.A. Enzyme Immobilization: The Quest for Optimum Performance. *Adv. Synth. Catal.* **2007**, *349*, 1289–1307. [CrossRef]

9.　Pellis, A.; Ferrario, V.; Cespugli, M.; Corici, L.; Guarneri, A.; Zartl, B.; Herrero Acero, E.; Ebert, C.; Guebitz, G.M.; Gardossi, L. Fully renewable polyesters via polycondensation catalyzed by Thermobifida cellulosilytica cutinase 1: An integrated approach. *Green Chem.* **2017**, *19*, 490–502. [CrossRef]

10.　Corici, L.; Ferrario, V.; Pellis, A.; Ebert, C.; Lotteria, S.; Cantone, S.; Voinovich, D.; Gardossi, L. Large scale applications of immobilized enzymes call for sustainable and inexpensive solutions: Rice husks as renewable alternatives to fossil-based organic resins. *RSC Adv.* **2016**, *6*, 63256–63270. [CrossRef]

11.　Contreras, L.M.; Schelle, H.; Sebrango, C.R.; Pereda, I. Methane potential and biodegradability of rice straw, rice husk and rice residues from the drying. *Water Sci. Technol.* **2012**, *65*, 1142–1149. [CrossRef] [PubMed]

12.　Available online: https://echa.europa.eu/regulations/reach (accessed on 23 March 2018).

13.　Wartelle, L.H.; Marshall, W.E. Quaternized agricultural by-products as anion exchange resins. *J. Environ. Manag.* **2005**, *78*, 157–162. [CrossRef] [PubMed]

14.　Prado, H.J.; Matulewicz, M.C. Cationization of polysaccharides: A path to greener derivatives with many industrial applications. *Eur. Polym. J.* **2014**, *52*, 53–75. [CrossRef]

15.　Sud, D.; Mahajan, G.; Kaur, M.P. Agricultural waste material as potential adsorbent for sequestering heavy metal ions from aqueous solutions—A review. *Bioresour. Technol.* **2008**, *14*, 6017–6602. [CrossRef] [PubMed]

16.　Tantrakulsiri, J.; Jeyashoke, N.; Krisanangkura, K.J. Utilization of rice hull ash as a support material for immobilization of Candida cylindracea lipase. *Am. Oil Chem. Soc.* **1997**, *74*, 173–175. [CrossRef]

17.　Park, B.; Wi, G.S.; Lee, H.K.; Singh, P.A.; Yoon, T.; Kim, S.Y. Characterization of anatomical features and silica distribution in rice husk using microscopic and micro-analytical techniques. *Biomass Bioenergy* **2003**, *25*, 319–327. [CrossRef]

18.　Coletta, C.V.; Rezende, V.C.; da Conceicao, F.R.; Polikarpov, I.; Giumaraes, G.E.F. Mapping the lignin distribution in pretreated sugarcane bagasse by confocal and fluorescence lifetime imaging microscopy. *Biotechnol. Biofuels* **2013**, *6*, 43. [CrossRef] [PubMed]

19.　Chen, B.; Hu, J.; Miller, M.E.; Xie, W.; Cai, M.; Gross, A.R. Candida antarctica lipase B chemically immobilized on epoxy-activated micro- and nanobeads: Catalysts for polyester synthesis. *Biomacromolecules* **2008**, *9*, 463–471. [CrossRef] [PubMed]

20.　Kodama, Y. Time Gating of Chloroplast Autofluorescence Allows Clearer Fluorescence Imaging in Planta. *PLoS ONE* **2016**, *11*, e0152484. [CrossRef] [PubMed]

21.　Schoevaart, R.; Siebum, A.; Van Rantwijk, F.; Sheldon, R.; Kieboom, T. Glutaraldehyde Cross-link Analogues from Carbohydrates. *Starch* **2005**, *57*, 161–165. [CrossRef]

22.　Kobayashi, M.; Takatsu, K. Cross-linked stabilization of trypsin with dextran-dialdehyde. *Biosci. Biotech. Biochem.* **1994**, *58*, 275–278. [CrossRef]

23.　Migneault, I.; Dartiguenave, C.; Bertrand, M.J.; Waldron, K.C. Glutaraldehyde: Behavior in aqueous solution, reaction with proteins, and application to enzyme crosslinking. *Biotechniques.* **2014**, *37*, 798–802. [CrossRef] [PubMed]

24.　Tashima, T.; Imai, M.; Kuroda, Y.; Yagi, S.; Nakagawa, T. Structure of a New Oligomer of Glutaraldehyde Produced by Aldol Condensation Reaction. *J. Org. Chem.* **1991**, *2*, 694–697. [CrossRef]

25.　Guigo, N.; Mazeau, K.; Putaux, J.L.; Heux, L. Surface modification of cellulose microfibrils by periodate oxidation and subsequent reductive amination with benzylamine: A topochemical study. *Cellulose* **2014**, *21*, 4119–4133. [CrossRef]

26.　Zhao, H.; Heindel, D.N. Determination of degree of substitution of formyl groups in polyaldehyde dextran by the hydroxylamine hydrochloride method. *Pharm. Res.* **1991**, *8*, 400–402. [CrossRef] [PubMed]

27.　Habibi, Y.; Chanzy, H.; Vignon, M.R. TEMPO-mediated surface oxidation of cellulose whiskers. *Cellulose* **2006**, *13*, 679–687. [CrossRef]

28.　Perez, S.D.; Montanari, S.; Vignon, M.R. TEMPO-mediated oxidation of cellulose III. *Biomacromolecules* **2003**, *4*, 1417–1425. [CrossRef] [PubMed]

29.　Monsan, P. Enzymes Immobilized on a Solid Support Containing Cellulose and Lignin. U.S. Patent 4405715, 20 September 1983.

30.　Pellis, A.; Corici, L.; Sinigoi, L.; D'Amelio, N.; Fattor, D.; Ferrario, V.; Ebert, C.; Gardossi, L. Towards feasible and scalable solvent-free enzymatic polycondensations: Integrating robust biocatalysts with thin film reactions. *Green Chem.* **2015**, *17*, 1756–1766. [CrossRef]

31. Corici, L.; Pellis, A.; Ferrario, V.; Ebert, E.; Cantone, S.; Gardossi, L. Understanding Potentials and Restrictions of Solvent-Free Enzymatic Polycondensation of Itaconic Acid: An Experimental and Computational Analysis. *Adv. Synth. Catal.* **2015**, *357*, 1763–1774. [CrossRef]

32. Ansorge-Schumacher, M.B.; Thum, O. Immobilised lipases in the cosmetics industry. *Chem. Soc. Rev.* **2013**, *42*, 6475–6490. [CrossRef] [PubMed]

33. Pellis, A.; Acero, E.H.; Gardossi, L.; Ferrario, V.; Guebitz, G.M. Renewable building blocks for sustainable polyesters: New biotechnological routes for greener plastics. *Polym. Int.* **2016**, *65*, 861–871. [CrossRef]

34. Pellis, A.; Guarneri, A.; Brandauer, M.; Herrero Acero, E.; Peerlings, H.; Gardossi, L.; Guebitz, G.M. Exploring mild enzymatic sustainable routes for the synthesis of bio-degradable aromatic-aliphatic oligoesters. *Biotechnol. J.* **2016**, *11*, 642–647. [CrossRef] [PubMed]

35. Robert, T.; Friebel, S. Itaconic acid—A versatile building block for renewable polyesters with enhanced functionality. *Green Chem.* **2016**, *18*, 2922–2934. [CrossRef]

36. Miller, L.M.; Mei, Y.; Gao, W.; Gross, R.A. Imaging the distribution of immobilized enzymes using infrared micro-spectroscopy. *Biomacromolecules* **2003**, *4*, 70–74. [CrossRef]

37. Hendriksen, H.V.; Kornbrust, B.A.; Ostergaard, P.R.; Stringer, M.A. Evaluating the Potential for Enzymatic Acrylamide Mitigation in a Range of Food Products Using an Asparaginase from Aspergillus oryzae. *J. Agric. Food Chem.* **2009**, *57*, 4168–4176. [CrossRef] [PubMed]

38. Wilson, K.M.; Rimm, E.B.; Thompson, K.M.; Mucci, L.A. Dietary acrylamide and cancer risk in humans: A review. *J. Verbrauch. Lebensm.* **2006**, *1*, 19–27. [CrossRef]

39. Teodor, E.; Litescu, S.C.; Lazar, V.; Somoghi, R. Hydrogel-magnetic nanoparticles with immobilized L-asparaginase for biomedical applications. *J. Mater. Sci. Mater. Med.* **2009**, *20*, 1307–1314. [CrossRef] [PubMed]

40. Kotzia, G.A.; Labrou, N.E. L-Asparaginase from Erwinia Chrysanthemi 3937: Cloning, expression and characterization. *J. Biotechnol.* **2006**, *127*, 657–669. [CrossRef] [PubMed]

41. Zhang, Y.Q.; Tao, M.L.; Shen, W.D.; Zhou, Y.Z.; Ding, Y.; Ma, Y.; Zhou, W.L. Immobilization of l-asparaginase on the microparticles of the natural silk sericin protein and its characters. *Biomaterials* **2004**, *25*, 3751–3759. [CrossRef] [PubMed]

42. Aung, H.P.; Bocola, M.; Schleper, S.; Röhm, K.H. Dynamics of a mobile loop at the active site of Escherichia coli asparaginase. *Biochim. Biophys. Acta* **2000**, *1481*, 349–359. [CrossRef]

43. Yao, M.; Yasutake, Y.; Morita, H.; Tanaka, I. Structure of the type I L-asparaginase from the hyperthermophilic archaeon Pyrococcus horikoshii at 2.16 Å resolution. *Acta Crystallogr. D* **2005**, *61*, 294–301. [CrossRef] [PubMed]

44. European Food Safety Authority. *Technical Report of EFSA: Explanatory Note on the Guidance of the Scientific Panel of Food Contact Material, Enzymes, Flavourings and Processing Aids (CEF) on the Submission of a Dossier on Food Enzymes*; EFSA Supporting Publication: Parma, Italy, 2014; EN-689; Available online: www.efsa.europa.eu (accessed on 28 July 2018).

45. Aghaiypour, K.; Wlodawer, A.; Lubkowski, J. Structural basis for the activity and substrate specificity of Erwinia chrysanthemi L-asparaginase. *Biochemistry* **2001**, *40*, 5655–5664. [CrossRef] [PubMed]

46. Ferrario, V.; Ebert, C.; Knapic, L.; Fattor, D.; Basso, A.; Spizzo, P.; Gardossi, L. Conformational changes of lipases in aqueous media: A comparative computational study and experimental implications. *Adv. Synth. Catal.* **2011**, *353*, 2466–2480. [CrossRef]

47. Basso, A.; Braiuca, P.; Cantone, S.; Ebert, C.; Linda, P.; Spizzo, P.; Caimi, P.; Hanefeld, U.; Degrassi, G.; Gardossi, L. In silico analysis of enzyme surface and glycosylation effect as a tool for efficient covalent immobilization of CalB and PGA on Sepabeads®. *Adv. Synth. Catal.* **2007**, *349*, 877–886. [CrossRef]